As in Section 6.14, alternative expressions for A' can be found in terms of potential temperature θ and concentration s (salinity or humidity). The conservation equations (4.1.8) and (4.1.9) now reduce for small perturbations to

$$\theta'' + h_* \, d\theta_0/dz_* = 0, \qquad s'' + h_* \, ds_0/dz_* = 0, \tag{6.18.9}$$

which have form similar to (6.14.11). However, θ'' is the perturbation from the equilibrium value at the same *pressure* and is not the same as θ'. In the case of a Lamb wave, for instance, for which the motion is purely horizontal, there is no change in potential temperature at any given level, so θ' vanishes; but since the pressure changes, θ'' is nonzero.

An alternative expression, obtained from (6.18.9) after use of (3.7.9) and (6.17.25), is

$$g(\alpha'\theta'' - \beta' s'')/N + N_* h_* = 0. \tag{6.18.10}$$

Substituting in (6.18.6) and using (6.17.28) and (6.17.22) at the surface give

$$A' = \iint \left\{ \frac{1}{2} \frac{p'(0)^2}{g\rho_r} + \int \frac{1}{2} \rho_* \left(\frac{g}{N}\right)^2 (\alpha'\theta'' - \beta' s'')^2 \, dz_* \right\} dx \, dy. \tag{6.18.11}$$

In the case of dry air ($s'' \equiv q'' = 0$) that is treated as a perfect gas, $\alpha' = 1/\theta_0$ by (3.7.14) and $N^2 = (g/\theta_0)\, d\theta_0/dz$ by (3.7.15). Using also the hydrostatic equation and the definition (6.17.8) of z_* to convert to pressure derivatives, and (6.17.22) for the definition of H_s, (6.18.11) becomes

$$A' = \iint \left\{ \frac{1}{2} \frac{p'(0)^2}{g\rho_r} + \int_0^{p_r} \frac{1}{2} \frac{\theta''^2}{(-g\rho\theta_0 \, d\theta_0/dp)} \, dp \right\} dx \, dy. \tag{6.18.12}$$

This is a form that is useful for calculating A' for the atmosphere, along with the perfect gas laws (3.1.2) and (3.7.4), which gives density ρ in terms of pressure and potential temperature, namely,

$$1/\rho = RT/p = R\theta p^{\kappa - 1}/p_r^{\kappa} \tag{6.18.13}$$

with κ given by (6.17.14). An expression in terms of temperature rather than potential temperature can be derived from this, or simply by substitution from (6.17.27) in (6.18.6) and using (6.18.2). Alternative forms follow from (6.17.25), the ideal gas equation (6.18.13), and expressions for N_* [see (6.17.24)] or N [see (6.14.4)]. Examples are

$$\begin{aligned} A' &= \iint \frac{1}{2} \frac{p'(0)^2}{g\rho_r} \, dx \, dy + \iiint \frac{1}{2} \frac{g^2 T_v''^2}{N^2 T_0^2} \, dM \\ &= \iint \frac{1}{2} \frac{p'(0)^2}{g\rho_r} \, dx \, dy + \iiint \frac{R\theta_0 T_v''^2 \, dM}{-2T_0 p \, d\theta_0/dp}. \end{aligned} \tag{6.18.14}$$

Expressions like this have been used to estimate the available potential energy of the atmosphere.

Chapter Seven

Effects of Rotation

7.1 Introduction

In the seventeenth century, a picture of how the atmosphere is set in motion began to emerge with Halley's (1686) work. However, arguments that neglected the rotation of the earth failed to explain the easterly component of the trade winds. Hadley (1735) showed how rotation (see Section 2.3) could explain this, using the concept of conservation of angular momentum. Laplace (1778-1779) recognized the importance of rotation in his theory of the tides and developed the necessary equations for studying rotation effects. Despite these equations being available for so many years, much of the work (based on these equations) that gives a proper foundation for the understanding of rotation effects is quite recent. One reason for the delay is the difficulty in setting up experiments like that of Marsigli in a rotating system [see, e.g., Saunders (1973)].

The problem that tells us a great deal about this question is the one discussed in Section 5.6, i.e., the one associated with Marsigli's experiment of adjustment of a fluid under gravity, but now with rotation effects included. The question of how a fluid, not initially in equilibrium, adjusts in a uniformly rotating system was not completely discussed until the time of Rossby (1938a), although transient wave solutions had been considered much earlier by Kelvin (Thomson, 1879). In a series of papers, Rossby (1936, 1937, 1938a,b, 1940; Rossby *et al.*, 1939) was concerned with how the mass and resulting pressure distributions in the ocean and atmosphere are established. In particular, he studied a problem in which momentum was supposed to be put into the ocean to give a nonequilibrium velocity distribution. Rossby (1938a) then considered the process of adjustment to equilibrium. A similar problem is introduced in the next section, and the rest of the chapter is devoted to the repercussions of this.

A key feature of the adjustment process in a rotating fluid is that the fluid adjusts rapidly (in a time of the order of the rotation period) to an equilibrium that is *not* a state of rest and contains more potential energy than does the rest state. In fact, very little of the potential energy initially present may be converted into kinetic energy. Also, the equilibrium state achieved (called a geostrophic equilibrium) cannot be found by solving the steady-state equations because these are degenerate in that any solution of the momentum equations satisfies the continuity equation exactly. It is this degeneracy, exemplified by the fact that the equilibrium fields of mass and momentum are related to each other, that causes the difficulties with which Rossby was concerned.

The equilibrium state achieved thus depends on the initial state, and Rossby showed the connection between the two states through conservation of a quantity he called potential vorticity. Using this property, the final state can be found, and this is shown in Section 7.2. Details of the transient motions require further analysis, and this is done in Section 7.3.

The analysis presented in this chapter is for a fluid that is rotating with uniform angular velocity about a vertical axis. However, application of the results to the atmosphere and ocean is possible in an approximate sense, and this point is discussed in Section 7.4. Section 7.5 is about the fundamental horizontal length scale that appears in problems dealing with adjustment under gravity of a rotating fluid. This is called the Rossby radius of deformation. Since the analysis can be applied to any of the normal modes of a stratified fluid, there is an infinite set of Rossby radii, one Rossby radius being associated with each of the modes.

The equilibrium solution is discussed in Sections 7.6 and 7.7. The large-scale motion in the ocean and atmosphere is nearly always close to such an equilibrium, and the implied connection between mass and velocity fields is of great importance in practice. In fact, much of our knowledge of the circulation of the ocean and atmosphere was deduced from the mass distribution before direct measurements were made. The relationship is used a great deal both as a means of estimating the velocity field and as an approximation in theoretical studies.

The discussion of energetics is taken up again in Section 7.8, which is concerned with the concept of available potential energy. This is the difference between the internal plus potential energy at any time and the minimum value to which it could be reduced by an inviscid isentropic rearrangement of fluid particles. The quantity is therefore a valuable measure of how much kinetic energy is potentially obtainable, and is widely used in studies of the circulation of the atmosphere and ocean.

Sections 7.9–7.12 are about the concept of vorticity and the results concerning circulation and potential vorticity that are of such great utility for rotating fluids. It is perhaps unfortunate that the name "potential vorticity" is given to more than one quantity, but in any given context it is usually quite clear which quantity is referred to! One form is that used for homogeneous shallow layers of fluid and the appropriate conservation equation is derived in Section 7.10. The potential vorticity in this case is defined as the total vorticity (assumed to be close to vertical) divided by the depth. A different form is appropriate in the continuously stratified case, and this is derived in Section 7.11. The conservation relation in this case requires no assumptions about the direction of the vorticity or about the ratio of horizontal to vertical scales, and the

conserved quantity is called Ertel's potential vorticity. Section 7.12 discusses the perturbation forms of the conservation equations for both types of potential vorticity. Finally, in Section 7.13 there is a discussion of an important practical problem for numerical weather prediction, namely, the initialization of fields, because this problem has much to do with the ideas developed in the remainder of the chapter.

7.2 The Rossby Adjustment Problem

In Section 5.6, the adjustment under gravity of a homogeneous shallow layer of fluid was considered, the particular case being one in which the fluid was initially at rest but had a discontinuity (or discontinuities) in surface level. Now the same problem will be considered for a rotating fluid, i.e., one that is initially at rest *relative to a frame of reference rotating with uniform angular velocity* $\frac{1}{2}f$ about a vertical axis. The motion is considered relative to this frame and is supposed to be a small perturbation from the state of relative rest at all times. The z axis is vertical; the bottom $z = -H$ is horizontal (i.e., a geopotential surface); and the surface elevation $z = \eta$ relative to a geopotential surface is assumed to be small. The horizontal scale is assumed to be large compared with the depth, so that the hydrostatic approximation can be made.

The equations are the same as those in Section 5.6 apart from the addition of the Coriolis acceleration $(-fv, fu)$, which produces the effects of rotation (see Section 4.5.1). Thus the momentum equation (4.10.11), after use of the hydrostatic equation [see (5.6.3)], gives

$$\partial u/\partial t - fv = -g\,\partial\eta/\partial x, \tag{7.2.1}$$

$$\partial v/\partial t + fu = -g\,\partial\eta/\partial y. \tag{7.2.2}$$

Since η is independent of z, the velocity (u, v) is independent of depth as in the nonrotating case. The letter f is used for *half* the rotation rate to avoid having factors of 2 appear in these equations. The continuity equation is (5.6.6), namely,

$$\partial\eta/\partial t + H(\partial u/\partial x + \partial v/\partial y) = 0. \tag{7.2.3}$$

The method of dealing with these equations in the nonrotating case was to take the divergence of the momentum equations [$\partial/\partial x$ of (7.2.1) plus $\partial/\partial y$ of (7.2.2)] and substitute from (7.2.3) for the horizontal divergence $\partial u/\partial x + \partial v/\partial y$. In the rotating case this gives

$$\partial^2\eta/\partial t^2 - c^2(\partial^2\eta/\partial x^2 + \partial^2\eta/\partial y^2) + fH\zeta = 0, \tag{7.2.4}$$

where c^2 is given by (5.5.4), namely,

$$c^2 = gH, \tag{7.2.5}$$

and

$$\zeta = \partial v/\partial x - \partial u/\partial y \tag{7.2.6}$$

is the *relative vorticity* of the fluid, i.e., the vertical component of the vorticity relative

to the rotating frame (the horizontal components are identically zero). When $f = 0$, this gives an equation in one variable η only, namely, the wave equation (5.6.10). In the rotating case, this equation points to the necessity of considering how the relative vorticity changes.

7.2.1 Conservation of Potential Vorticity

Equations (7.2.1)–(7.2.3) were given by Kelvin (Thomson, 1879) in his paper "On gravitational oscillations of rotating water," in which he sought to simplify Laplace's tidal theory by considering "an area of water so small that the equilibrium figure of its surface is not sensibly curved." From these equations he derived an equation that is of fundamental importance in the theory of rotating fluids. This is obtained in two steps. First, the curl of the momentum equations $[\partial/\partial y$ of (7.2.1) minus $\partial/\partial x$ of (7.2.2)] eliminates η and gives the vorticity equation

$$\partial\zeta/\partial t + f(\partial u/\partial x + \partial v/\partial y) = 0, \tag{7.2.7}$$

i.e., the rate of change of ζ/f is equal to minus the horizontal divergence. Second, the continuity equation (7.2.3) is used to eliminate the horizontal divergence, to give

$$\frac{\partial}{\partial t}\left(\frac{\zeta}{f} - \frac{\eta}{H}\right) = 0. \tag{7.2.8}$$

The fact that this equation is easily integrated with respect to time is a very powerful result. Equation (7.2.8) is in fact a linearized form of the equation (to be considered later) expressing the conservation of *potential vorticity* for a homogeneous rotating fluid. The quantity Q', defined by

$$Q' = \zeta/H - f\eta/H^2, \tag{7.2.9}$$

may be called the perturbation potential vorticity, and (7.2.8) expresses the fact that Q' retains its initial value at each point for all time, i.e.,

$$Q'(x, y, t) = Q'(x, y, 0). \tag{7.2.10}$$

This infinite memory of an inviscid rotating fluid can be exploited, as will be shown, to find the final equilibrium solution for a particular initial state *without considering* details of the transient motion at finite times. Kelvin (Thomson, 1879), being interested only in oscillations, took Q' to be zero, whereas the most interesting cases of adjustment to equilibrium are those for which Q' is nonzero. Solutions with nonzero Q' were apparently not considered until the time of Rossby (1938a).

The particular initial condition to be considered here is the same as that in Section 5.6, namely, $u = v = 0$ and surface elevation given by (5.6.13), i.e.,

$$\eta = -\eta_0 \operatorname{sgn}(x). \tag{7.2.11}$$

(This is an initial condition different from that considered by Rossby, but the analysis is similar.) The integral of (7.2.8) in this case is

$$\zeta/f - \eta/H = (\eta_0/H) \operatorname{sgn}(x), \tag{7.2.12}$$

and substitution in (7.2.4) gives an equation for η alone, namely,

$$\partial^2\eta/\partial t^2 - c^2(\partial^2\eta/\partial x^2 + \partial^2\eta/\partial y^2) + f^2\eta = -fH^2Q'(x, y, 0)$$
$$= -f^2\eta_0 \operatorname{sgn}(x). \tag{7.2.13}$$

7.2.2 The Steady Solution: Geostrophic Flow

If the gravitational adjustment processes lead ultimately to a steady state, that state will be given by the time-independent solution of (7.2.13). Since the initial condition is independent of y, the solution at all subsequent times can be assumed to be independent of y, and thus the vorticity ζ is equal to $\partial v/\partial x$. Furthermore, a steady solution of (7.2.1) and (7.2.2) must entail a balance between the Coriolis acceleration $(-fv, fu)$ and the pressure gradient. This is known as a *geostrophic balance*

$$fu = -g\,\partial\eta/\partial y, \qquad fv = g\,\partial\eta/\partial x, \tag{7.2.14}$$

and has the property that the flow is along contours of constant pressure (i.e., along isobars, as is familiar from weather maps).

The steady-state solution has a very special property in that *any* solution satisfying the geostrophic balance happens to satisfy the time-independent version of the continuity equation (7.2.3) *exactly*, i.e., is nondivergent with

$$\partial u/\partial x + \partial v/\partial y = 0. \tag{7.2.15}$$

An alternative way of viewing this result is to use (7.2.15) to introduce a stream function ψ such that

$$u = -\partial\psi/\partial y, \qquad v = \partial\psi/\partial x. \tag{7.2.16}$$

Then the geostrophic balance may be written

$$f\,\partial\psi/\partial y = g\,\partial\eta/\partial y, \qquad f\,\partial\psi/\partial x = g\,\partial\eta/\partial x. \tag{7.2.17}$$

If η is eliminated from this pair of equations in order to obtain an equation for ψ, i.e., if the y derivative of the second equation is subtracted from the x derivative of the first, all that emerges is the trivial statement that zero equals zero. In fact (7.2.17) shows that the stream function (with suitable choice of reference value) is related to pressure perturbation by

$$f\psi = g\eta = p'/\rho. \tag{7.2.18}$$

Any distribution $\eta(x, y)$ of surface elevation gives a stream function ψ by (7.2.18) that satisfies all the steady-state equations.

In this sense, the steady-state equations are *degenerate* and cannot yield the ultimate steady solution by themselves. An added piece of information is required, and this is the fact that each element of fluid retains its initial potential vorticity, i.e., (7.2.10) is satisfied, which, for the special case being considered, takes the form (7.2.12). For a geostrophically balanced flow, substitution of (7.2.14) in (7.2.6) shows that the vorticity is given by

$$\zeta = f^{-1}g(\partial^2\eta/\partial x^2 + \partial^2\eta/\partial y^2), \tag{7.2.19}$$

and so (7.2.9) and (7.2.10) yield the steady-state version of (7.2.13),

$$-c^2(\partial^2\eta/\partial x^2 + \partial^2\eta/\partial y^2) + f^2\eta = -fH^2Q'(x, y, 0). \tag{7.2.20}$$

For the present case, this gives

$$-c^2\, d^2\eta/dx^2 + f^2\eta = -f^2\eta_0\,\mathrm{sgn}(x). \tag{7.2.21}$$

The solution η that is continuous and antisymmetric about $x = 0$ is given by

$$\frac{\eta}{\eta_0} = \begin{cases} -1 + e^{-x/a} & \text{for} \quad x > 0 \\ 1 - e^{x/a} & \text{for} \quad x < 0, \end{cases} \tag{7.2.22}$$

where

$$a = c/|f| = (gH)^{1/2}/|f| \tag{7.2.23}$$

is a length scale of fundamental importance for the behavior of rotating fluids subject to gravitational restoring forces. It is called the Rossby *radius of deformation*, following the name given by Rossby (1938a, p. 242), or simply the "Rossby radius" or the "radius of deformation." The modulus sign is used in (7.2.23) to ensure that a be a positive quantity since f can have either sign.

The velocity field associated with the solution (7.2.22) follows from the geostrophic equation (7.2.14), which gives $u = 0$ and

$$v = -(g\eta_0/fa)\exp(-|x|/a). \tag{7.2.24}$$

The flow is *not* in the direction of the pressure gradient, but at right angles, i.e., along contours of surface elevation that are parallel to the line of the initial discontinuity. The solution is depicted in Fig. 7.1.

7.2.3 Energy Considerations

The energy equations for rotating shallow-water motion may be found by the same methods as those in Section 5.7. In particular, the mechanical energy equation is

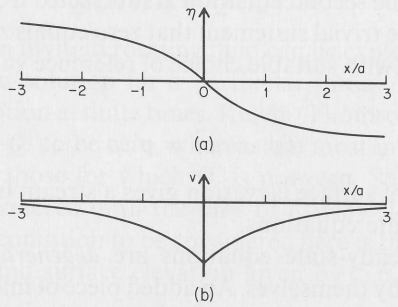

Fig. 7.1. The geostrophic equilibrium solution corresponding to adjustment from an initial state that is one of rest but has uniform infinitesimal surface elevation $-\eta_0$ for $x > 0$ and elevation η_0 for $x < 0$. (a) The equilibrium surface level η, which tends toward the initial level as $x \to \pm\infty$. The unit of distance in the figure is the Rossby radius $a = (gH)^{1/2}/f$, where g is the acceleration due to gravity, H the depth of fluid, and f twice the rate of rotation of the system about a vertical axis. (b) The corresponding equilibrium velocity distribution, there being a "jet" directed *along* the initial discontinuity in level with maximum velocity equal to $(g/H)^{1/2}$ times η_0.

obtained by adding ρHu times (7.2.1) to ρHv times (7.2.2). This operation *eliminate* the terms that come from the Coriolis acceleration, so that rotation terms do no appear *explicitly* in the energy equations, which therefore have exactly the same form as those in Section 5.7. However, the solution of the adjustment problem is drastically affected by rotation, and thus the energy changes in the rotating case are quite different from those of the nonrotating case discussed in Section 5.7.

Consider first the perturbation potential energy. This is infinite at the initial moment but, unlike the nonrotating case, it is *still* infinite when the steady equilibrium solution is established (assuming such an equilibrium does occur). However, the *change* in potential energy per unit length is finite and is given by

$$\text{P.E. released per unit length} = 2\cdot\tfrac{1}{2}\rho g\eta_0^2\int_0^\infty \{1 - (1 - e^{-x/a})^2\}\,dx$$

$$= \tfrac{3}{2}\rho g\eta_0^2 a. \tag{7.2.25}$$

In the nonrotating case, *all* the potential energy available in the initial perturbation is converted into kinetic energy. For the rotating case, only a finite amount of potential energy is released. The amount of kinetic energy per unit length found in the equilibrium solution is given by

$$\text{K.E. per unit length} = 2\cdot\tfrac{1}{2}\rho Hg^2\eta_0^2(fa)^{-2}\int_0^\infty e^{-2x/a}\,dx$$

$$= \tfrac{1}{2}\rho g\eta_0^2 a. \tag{7.2.26}$$

This is only one-third of the potential energy released! What happens to the other two-thirds? Rossby (1938a, p. 244) suggested that a fluid particle must "continue its displacement beyond the equilibrium point until an excessive pressure gradient develops which forces it back. An *inertia* oscillation around the equilibrium position results." These speculative comments are fairly close to the truth, but give the mistaken impression that an equilibrium solution is never reached in any finite domain. What really happens will be found in Section 7.3, where details of the transients will be calculated.

7.2.4 Summary

The problem considered above, even though only partially completed, gives a great many insights into the behavior of rotating fluids responding to gravitational forces. Five notable features are listed below, and various concepts arising from these results are discussed in more detail in later sections of this chapter.

(a) The energy analysis indicates that *energy is hard to extract* from a rotating fluid. In the problem studied, there was an infinite amount of potential energy available for conversion into kinetic energy, but only a finite amount of this available energy was released. The reason was that a geostrophic equilibrium was established and such an equilibrium retains potential energy—an infinite amount in the case studied!

(b) The steady equilibrium solution is *not* one of rest, but is a *geostrophic balance*

i.e., a balance between the Coriolis acceleration and the pressure gradient divided by density.

(c) The steady solution is *degenerate* in the sense that any velocity field in geostrophic balance satisfies the continuity equation exactly. Therefore the steady solution cannot be found by looking for a solution of the steady-state equations—some other item of information is required.

(d) This information is supplied by the conservation of potential vorticity principle, i.e., the potential vorticity of each fluid element is the same as that at the initial instant. With this knowledge, a steady solution can be found.

(e) The equation determining this steady solution contains a length scale a, called the Rossby radius of deformation, which is equal to $c/|f|$, where c is the wave speed in the absence of rotation effects, i.e., $(gH)^{1/2}$. If f tends to zero, a tends to infinity, indicating that for length scales small compared with a, rotation effects are small, whereas for scales comparable with or large compared with a, rotation effects are important.

7.3 The Transients

To complete the solution of the adjustment problem, i.e., of (7.2.13), it is necessary to add a solution of the homogeneous equation

$$\partial^2\eta/\partial t^2 - c^2(\partial^2\eta/\partial x^2 + \partial^2\eta/\partial y^2) + f^2\eta = 0 \tag{7.3.1}$$

to a particular solution, which can be taken as the steady solution $\eta_{\text{steady}}(x)$, given by (7.2.22). The solution of (7.3.1) must satisfy the initial condition

$$\eta = -\eta_0 \operatorname{sgn}(x) - \eta_{\text{steady}},$$

i.e.,

$$\eta = -\eta_0 e^{-|x|/a} \operatorname{sgn}(x) \qquad \text{at} \quad t = 0. \tag{7.3.2}$$

Equation (7.3.1) is sometimes known as the Klein–Gordon equation (Morse and Feshbach, 1953) because of applications in physics, and Morse and Feshbach discuss an analog provided by a stretched string embedded in a rubberized medium. The equation is also discussed by Whitham (1974). The transient solution for Rossby's original problem was found by Cahn (1945) and is discussed by Blumen (1972).

Equation (7.3.1) has wavelike solutions of the form

$$\eta \propto \exp i(kx + ly - \omega t), \tag{7.3.3}$$

which on substitution in (7.3.1) gives the dispersion relation

$$\omega^2 = f^2 + \kappa_H^2 c^2, \tag{7.3.4}$$

where

$$\kappa_H^2 = k^2 + l^2 \tag{7.3.5}$$

is the square of the horizontal wavenumber. Waves with this dispersion relation (k, l real) will be referred to as "Poincaré waves" here, although this name is sometimes reserved for the subset that satisfies the boundary conditions for a channel (see

Chapter 10). Despite the name, such waves were first discussed by Kelvin (Thomson, 1879). In meteorology, they are usually referred to simply as gravity waves, with rotation effects being understood. A graph of the dispersion relation is shown in Fig. 7.2. It can be seen from the dispersion relation that the properties of these waves depend on how the wavelength compares with the Rossby radius. The limiting cases are as follows:

(i) Short waves ($\kappa_H a \gg 1$), i.e., waves short compared with the Rossby radius, for which (7.3.4) becomes approximately

$$\omega \sim \kappa_H c; \tag{7.3.6}$$

hence "short" waves are ordinary nondispersive shallow-water waves. It will be recalled, however, that shallow-water theory requires that the waves have horizontal scale large compared with the depth, so these waves have the above form only when the Rossby radius is large compared with the depth. This condition is satisfied in the atmosphere and ocean (see Section 7.4).

(ii) Long waves ($\kappa_H a \ll 1$), i.e., waves long compared with the Rossby radius, for which (7.3.4) gives approximately

$$\omega \sim f, \tag{7.3.7}$$

i.e., the frequency is approximately constant and equal to f or twice the rotation rate. In this limit, gravity has no effect, so fluid particles are moving under their own inertia. For this reason f is often called the "*inertial*" *frequency*.

The group velocity $\mathbf{c}_g$ of Poincaré waves is equal to the slope of the dispersion curve in Fig. 7.2 and thus has a maximum value of c obtained in the shortwave limit, whereas it tends to zero as the wavelength tends to infinity. The consequences of

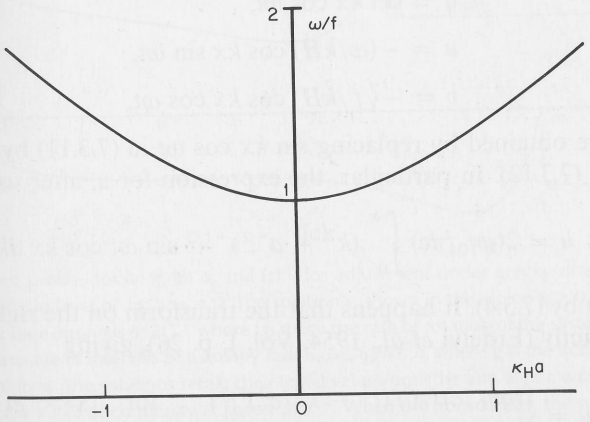

Fig. 7.2. The dispersion relation for Poincaré waves. For small wavenumber κ_H (waves long compared with the Rossby radius a), the frequency ω is only slightly above the "inertial" frequency f. For large wavenumber (waves short compared with the Rossby radius), the waves are little affected by rotation and so approximate the nondispersive shallow-water waves found in a nonrotating system. Note that the group velocity, which is the gradient of the curve shown in the figure, is zero for zero wavenumber (infinitely long waves) and increases monotonically in magnitude with κ_H to a maximum of $(gH)^{1/2}$ for very short waves.

these variations will be seen in the transient solution because short waves move off rapidly from the initial discontinuity, whereas long waves move off only slowly—the longer the wave, the smaller the group velocity, which velocity is given by

$$\mathbf{c}_g = c^2\mathbf{k}/\omega \approx c^2\mathbf{k}/f \qquad \text{for small } \mathbf{k}. \tag{7.3.8}$$

Other properties of Poincaré waves are discussed later.

The solution of the transient problem can now be found by finding a suitable superposition of wave solutions (7.3.3) (Gill, 1976). The appropriate combination of waves is the one that gives the initial distribution (7.3.2), and this can be found from tables of integral transforms [see, e.g., Erdélyi *et al.* (1954, Vol. I, p. 72)]. Thus (7.3.2) is equivalent to

$$\eta = -\frac{2\eta_0}{\pi}\int_0^\infty \frac{k \sin kx}{k^2 + a^{-2}}\,dk. \tag{7.3.9}$$

At later times, η will consist of the same superposition of Poincaré waves, but allowance must be made for their propagation. Thus 2 sin kx in (7.3.9) will be replaced by the combination of Poincaré waves that preserves antisymmetry, namely,

$$\sin(kx + \omega t) + \sin(kx - \omega t) = 2 \sin kx \cos \omega t. \tag{7.3.10}$$

In other words, the solution at time t is given by

$$\eta = -\frac{2\eta_0}{\pi}\int_0^\infty \frac{k \sin kx \cos \omega t}{k^2 + a^{-2}}\,dk, \tag{7.3.11}$$

where ω is given by (7.3.4) with $l = 0$.

The solutions for u and v can also be obtained by reference to the standing-wave solutions that follow directly from Eqs. (7.2.2) and (7.2.3) with $\partial/\partial y = 0$, namely,

$$\begin{aligned} \eta &= \sin kx \cos \omega t, \\ u &= -(\omega/kH) \cos kx \sin \omega t, \\ v &= -(f/kH) \cos kx \cos \omega t. \end{aligned} \tag{7.3.12}$$

Thus u and v are obtained by replacing sin kx cos ωt in (7.3.11) by the appropriate expression from (7.3.12). In particular, the expression for u, after use of (7.3.4), is

$$u = 2(g\eta_0/\pi c)\int_0^\infty (k^2 + a^{-2})^{-1/2} \sin \omega t \cos kx\,dk, \tag{7.3.13}$$

where ω is given by (7.3.4). It happens that the transform on the right-hand side can be evaluated exactly (Erdélyi *et al.*, 1954, Vol. I, p. 26), giving

$$u = \begin{cases} (g\eta_0/c)J_0(f(t^2 - x^2/c^2)^{1/2}) & \text{for } |x| < ct \\ 0 & \text{for } |x| > ct, \end{cases} \tag{7.3.14}$$

where J_0 is a Bessel function of order zero. This is a special solution of the Klein–Gordon equation, corresponding to a point impulse at $x = 0$ and $t = 0$ (Morse and Feshbach, 1953, p. 139), i.e., the acceleration $\partial u/\partial t$ has the form of a delta function as a result of the infinite pressure gradient that exists at the initial instant. The solution

(7.3.14) is useful for computing solutions, and integrals for η, v in terms of the Bessel function can be obtained from (7.2.2) and (7.2.3). Cahn (1945) used expressions of this type for Rossby's initial values.

The solutions for η, u, v are displayed in Fig. 7.3 and can be compared with the solutions for the nonrotating case discussed in Section 5.6 (see Fig. 5.9a). Instead of the wave front transmitting just the initial step, as in the nonrotating case, the step is now followed by a "wake" of waves that trail behind because of dispersion. The short waves that make up the step still travel at speed c, but longer waves travel more slowly (i.e., their group velocity is smaller), so they lag behind the front. At a fixed point, this is made evident by the fact that the frequency appears to decrease with time after the wave front has passed (i.e., the time between wave crests increases) and soon approaches the inertial frequency f, as can be seen from (7.3.14). Figure 7.4b shows how u changes with time at $x = a$. Another property that can be seen from

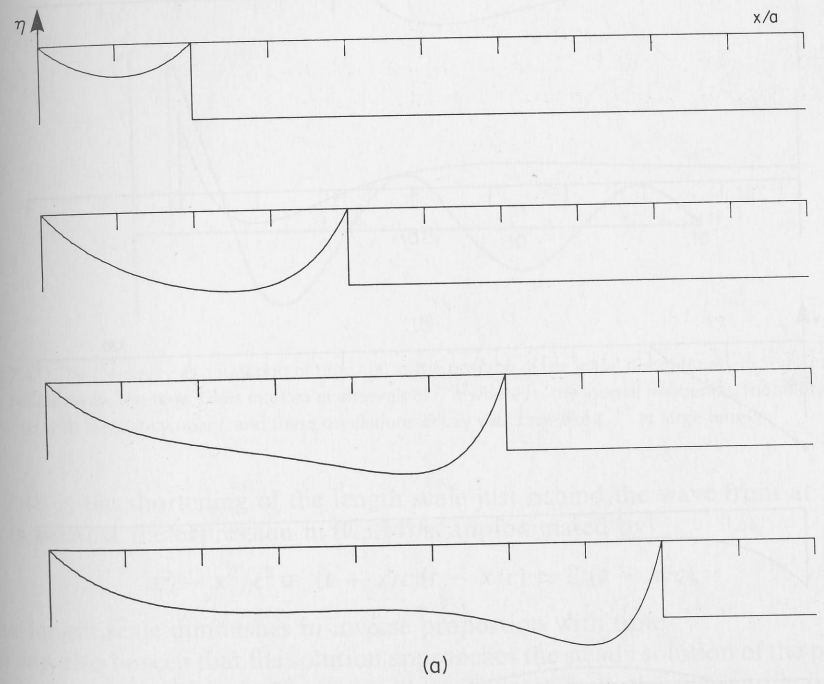

Fig. 7.3. Transient profiles for (a) η, (b) u, and (c) v for adjustment under gravity of a fluid with an initial infinitesimal discontinuity in level of $2\eta_0$ at $x = 0$. The solution is shown in the region $x > 0$, where the surface was initially depressed, at time intervals of $2f^{-1}$, where f is twice the rate of rotation of the system about a vertical axis. The marks on the x axis are at intervals of a Rossby radius, i.e., $(gH)^{1/2}/f$, where g is the acceleration due to gravity and H is the depth of fluid. The solutions retain their initial values until the arrival of a wave front that travels out from the position of the initial discontinuity at speed $(gH)^{1/2}$. When the front arrives, the surface elevation rises by η_0 and the u component of velocity rises by $(g/H)^{1/2}\eta_0$ just as in the nonrotating case depicted in Fig. 5.9a. This is because the first waves to arrive are the very short waves, which are unaffected by rotation. Behind the front, however, is a "wake" of waves produced by dispersion, which in the case of u, have the slope given by the Bessel function (7.3.14). This is the point impulse solution to the Klein–Gordon equation. The "width" of the front narrows in inverse proportion with time. Well behind the front, the solution adjusts to the geostrophic equilibrium solution depicted in Fig. 7.1.

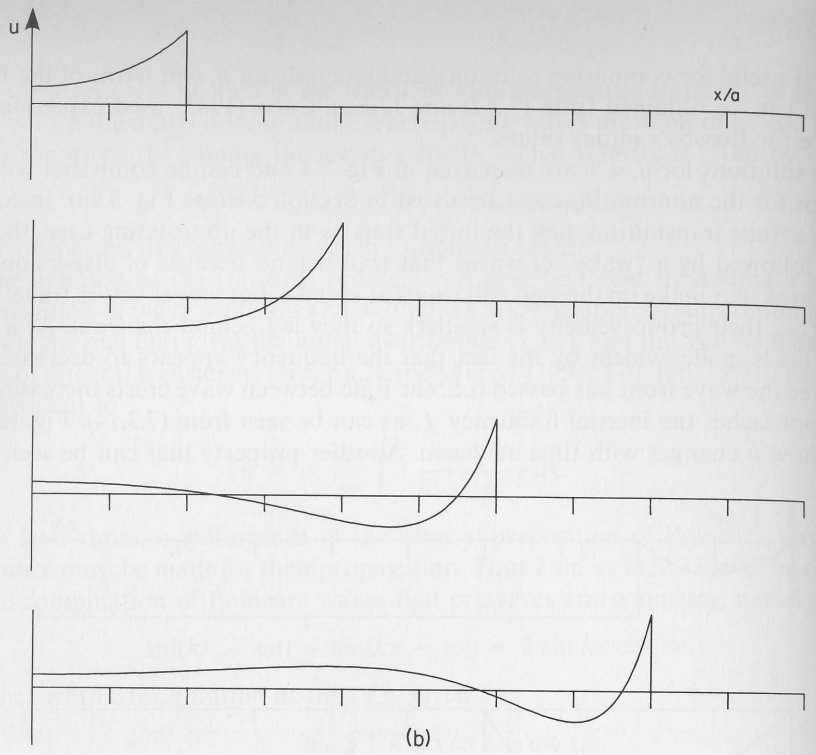

(b)

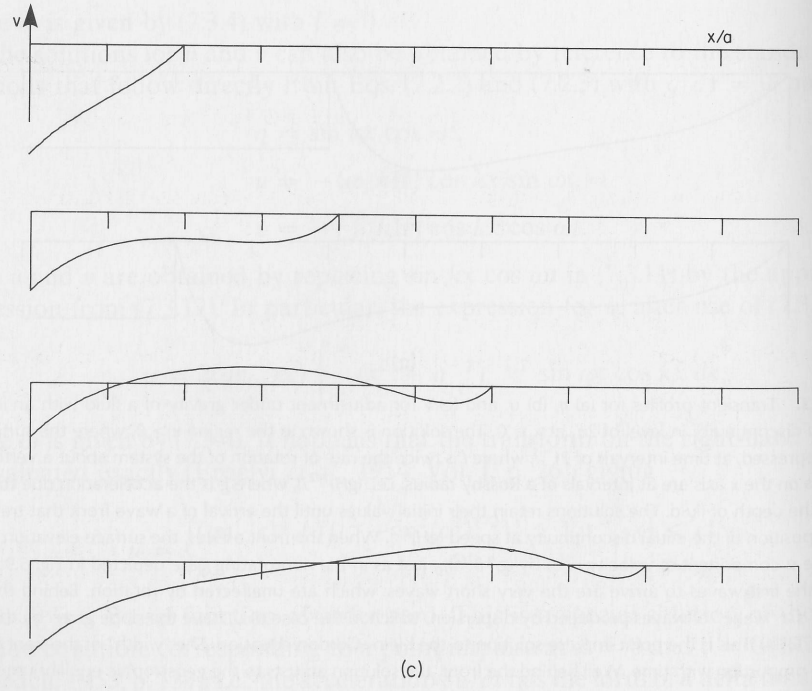

(c)

Fig. 7.3. *(continued)*

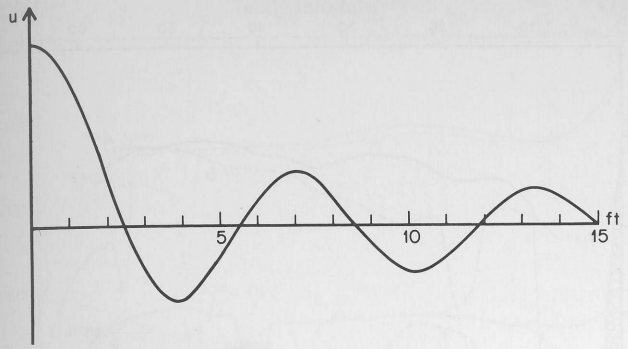

(a)

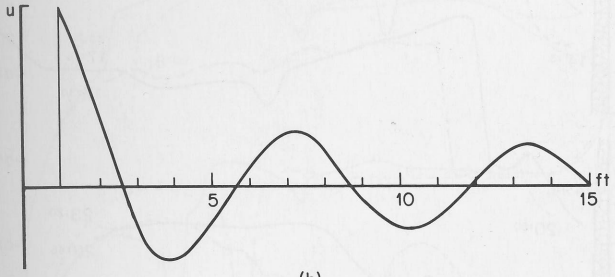

(b)

Fig. 7.4. The u velocity as a function of time t (a) at the position of the initial discontinuity in level and (b) o Rossby radius away. The time axis is marked at intervals of f^{-1}, where f is the inertial frequency. The solutions sh oscillations with frequency near f, and these oscillations decay with time like $t^{-1/2}$ at large times.

Fig. 7.4b is the shortening of the length scale just behind the wave front at $x =$ This is because the expression in (7.3.14) is approximated by

$$t^2 - x^2/c^2 \equiv (t + x/c)(t - x/c) \simeq 2t(t - x/c),$$

so the length scale diminishes in inverse proportion with time.

It can also be seen that the solution approaches the steady solution of the previo paragraph as time goes on. Details can be calculated from the asymptotic behavi of the Bessel function for large times. It is also clear where the potential energy th was not converted into kinetic energy of the equilibrium solution has gone. The wa fronts moving away from the initial discontinuity carry energy with them, so for a finite region energy is lost through the sides by "radiation" of Poincaré waves un the only energy left is that associated with the steady geostrophic equilibrium.

The other new information provided by the transient solution is the *time scale* the adjustment process. Near the origin, i.e., within a distance of the order of t Rossby radius, the time scale is f^{-1}, i.e., the rotation time scale or "inertial" time sca $(2\pi/f$ is also half the period of a Foucault pendulum). However, as Rossby suggeste the solution does not adjust monotonically to the equilibrium solution, but oversho

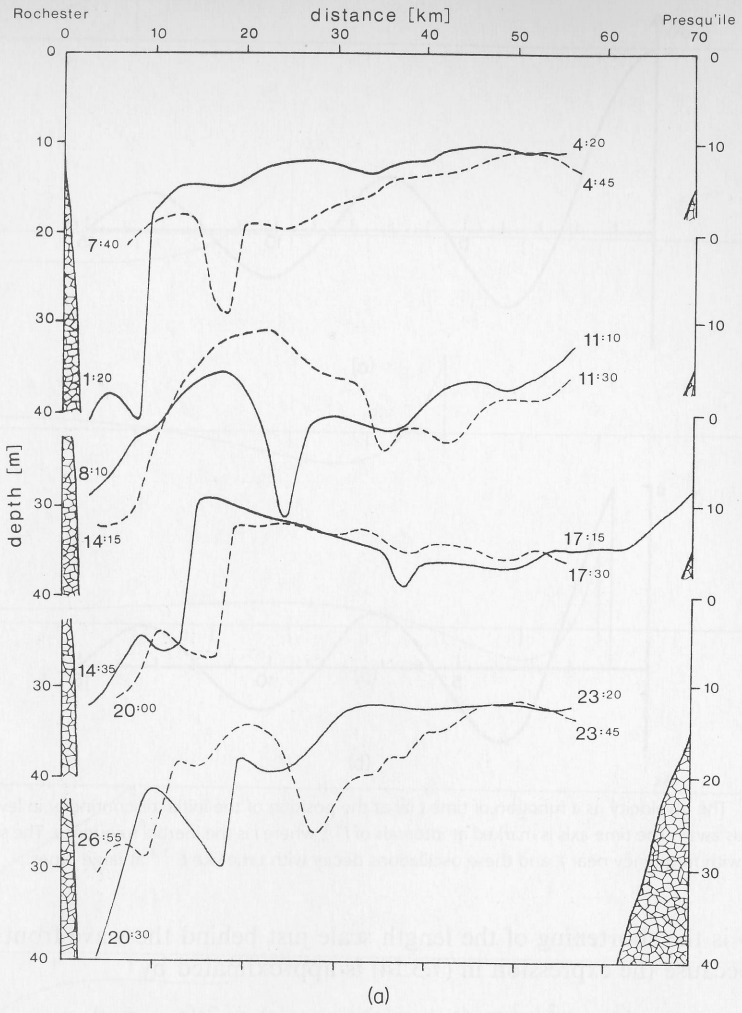

Fig. 7.5. (a) An (internal) Poincaré wave front observed in Lake Ontario following a storm on 9 August 1972. Lines show the thermocline depth as measured by the 10° isotherm. Times of the beginning and end of each transect are shown. The first transect shows the large downwelling produced by the passage of the storm, and subsequent sections show the geostrophic adjustment process involving radiation of Poincaré waves. (b) Results of a (nonlinear two-layer) model simulation of this event by Simons (1978). The diagrams are from Simons (1978, 1980) and may be compared with the solution shown in Fig. 7.3 for a very simple initial condition.

and tends to oscillate about it. The behavior is typified by the value of u at $x = 0$, namely,

$$u = (g\eta_0/c)J_0(ft), \tag{7.3.15}$$

shown in Fig. 7.4a. For large ft, this solution is approximated asymptotically by

$$u \sim (g\eta_0/c)(2/\pi ft)^{1/2} \sin(ft + \pi/4). \tag{7.3.16}$$

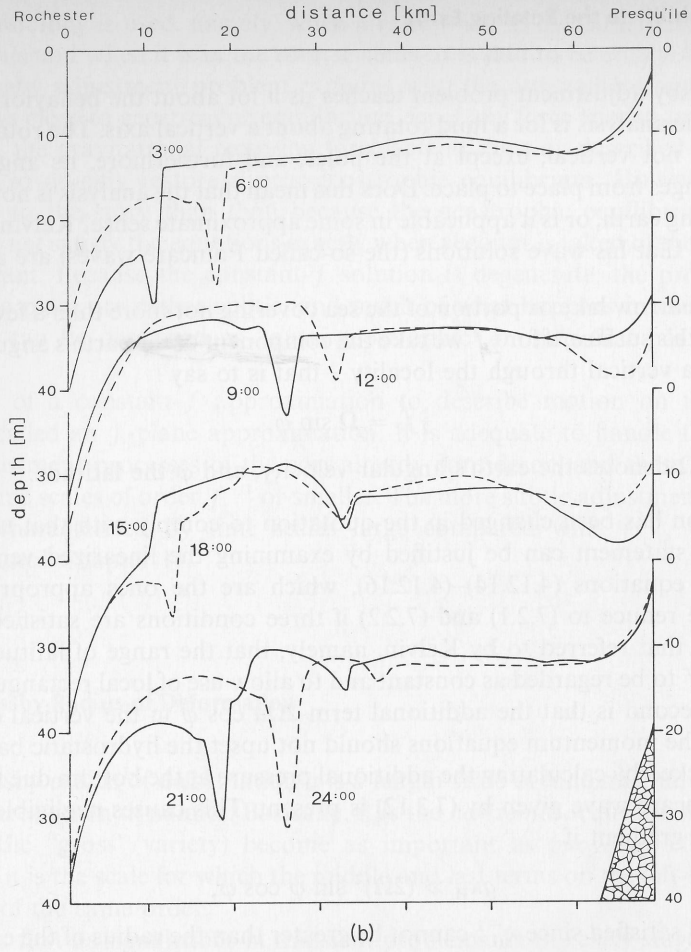

Fig. 7.5. (*continued*)

Thus oscillations of frequency f are found because these are associated with the lon waves of zero group velocity that are left behind. However, the group velocity is nc exactly zero for any nonzero wavenumber, so energy disperses slowly and this cause the algebraic decay in the oscillations as given by (7.3.16).

Some waves with characteristics very similar to those depicted in Figs. 7.3 an 7.4 were observed in Lake Ontario in August 1972 and are shown in Fig. 7.5. Th initial condition, produced by storm-induced downwelling near the boundary, has steplike structure as assumed for the solution shown in Figs. 7.3 and 7.4. Howeve because of the boundary at the coast, these are also reflected waves. A linear calcula tion could easily deal with them by the method of images used to construct Fig. 5.9 in the nonrotating case. The model solution shown in Fig. 7.5b includes nonlinear an other effects as well.

7.4 Applicability to the Rotating Earth

The Rossby adjustment problem teaches us a lot about the behavior of rotating fluids, but the analysis is for a fluid rotating about a vertical axis. The rotation axis of the earth is not vertical, except at the poles, and furthermore, its angle with the vertical changes from place to place. Does this mean that the analysis is not applicable to the rotating earth, or is it applicable in some approximate sense? Kelvin (Thomson, 1879) stated that his wave solutions (the so-called Poincaré waves) are applicable

> in any narrow lake or portion of the sea covering not more than a few degrees of the earth's surface, if for $\frac{1}{2}f$ we take the component of the earth's angular velocity round a vertical through the locality—that is to say
>
> $$\tfrac{1}{2}f = \Omega \sin \varphi, \tag{7.4.1}$$
>
> where Ω denotes the earth's angular velocity, and φ the latitude.

(The notation has been changed in the quotation to comply with that used here.)

Kelvin's statement can be justified by examining the linearized version of the momentum equations (4.12.14)–(4.12.16), which are the ones appropriate to the earth. These reduce to (7.2.1) and (7.2.2) if three conditions are satisfied. The first condition is that referred to by Kelvin, namely, that the range of latitude be small enough for f to be regarded as constant and to allow use of local rectangular coordinates. The second is that the additional term $2\Omega u \cos \varphi$ in the vertical component (4.12.16) of the momentum equations should not upset the hydrostatic balance. This is easily checked by calculating the additional pressure at the bottom due to this term when a Poincaré wave given by (7.3.12) is present. This causes negligible change in the pressure gradient if

$$g\kappa_H \gg (2\Omega)^2 \sin \varphi \cos \varphi, \tag{7.4.2}$$

which is well satisfied since κ_H^{-1} cannot be greater than the radius of the earth, which happens to be much smaller than

$$g/(2\Omega)^2 \simeq 460{,}000 \quad \text{km}.$$

The third condition is that it be possible to neglect the additional term $2\Omega w \cos \varphi$ in the horizontal momentum equation. The largest value of w is its value $\partial\eta/\partial t$ at the surface. Using the Poincaré wave solution (7.3.12), it is found that the condition for its neglect is that

$$H\kappa_H \ll \tan \varphi, \tag{7.4.3}$$

which is implied by the condition $H\kappa_H \ll 1$, used already to justify the hydrostatic approximation, provided φ is not too small, i.e., the area considered is not too close to the equator.

Further discussion of the approximation will be made later. For the moment, the main point is that f is interpreted as the quantity defined by (7.4.1), which is called the *Coriolis parameter*. This parameter is positive in the northern hemisphere and negative in the southern hemisphere. The sign of f is very important in many applications, so

special terminology is used, namely, when a rotation is in the same sense as f, it is called *cyclonic* and when it is in the reverse sense, it is said to be *anticyclonic*.

The Rossby adjustment problem explains why the atmosphere and ocean are nearly always close to geostrophic equilibrium, for if any force tries to upset such an equilibrium, the gravitational restoring force acts in the way described in Sections 7.2 and 7.3 to quickly restore a near-geostrophic equilibrium. However, there is much more to the story than that, because the geostrophic equilibrium solution (7.2.14) does *not* satisfy the equations exactly when account is taken of the fact that f is not constant. Because the constant-f solution is degenerate, the processes that actually take place are rather subtle, and much of what happens in the ocean and atmosphere can be described as "quasi-geostrophic" motion that has this subtle character.

The use of a constant-f approximation to describe motion on the earth is sometimes called an f-plane approximation. It is adequate to handle the rapid or "gross" adjustment processes of the sort already considered, and these are characterized by time scales of order f^{-1} or smaller. The more subtle adjustment processes, which are characterized by time scales large compared with f^{-1}, will not be considered until Chapter 11.

7.5 The Rossby Radius of Deformation

The Rossby radius of deformation a is a length scale of fundamental importance in atmosphere–ocean dynamics. Basically, it is the *horizontal scale* at which *rotation* effects (of the "gross" variety) become as important as *buoyancy* effects. More specifically, it is the scale for which the middle and last terms on the left-hand side of (7.2.13) are of the same order.

Consider first its significance in transient problems. In the early stages of adjustment from an initial discontinuity, the change of level is confined to a small distance, the pressure gradient is consequently very large, and gravity dominates the behavior. In other words, at scales small compared with the Rossby radius, the adjustment is approximately the same as in a nonrotating system. Later, however, when the change in level is spread over a distance comparable with the Rossby radius, the Coriolis acceleration becomes just as important as the pressure gradient term and thus rotation causes a response that is markedly different from the nonrotating case.

The same considerations apply to Poincaré waves, so the short waves ($\kappa_H^{-1} \ll a$) are very much like gravity waves in a nonrotating system, as discussed in Section 7.3. For waves with scales comparable with the radius of deformation, the buoyancy term $\kappa_H^2 c^2$ in the dispersion relation (7.3.4) is of the same order as the rotation term f^2. Long waves ($\kappa_H^{-1} \gg a$), on the other hand are *dominated* by rotation effects and have frequency close to the inertial frequency f, which for applications to the ocean and atmosphere is also the Coriolis parameter given by (7.4.1). The inertial period $2\pi/f$ is also half the period of a Foucault pendulum, and therefore is sometimes called a half pendulum day. This varies with latitude and is 12 hr at the poles, 17 hr

at 45° latitude, 1 day at 30°, and nearly 3 days at 10°. At the equator, it becomes infinite, but by that stage the f-plane approximation breaks down.

The Rossby radius of deformation is not only significant for the behavior of transients, but is also an important scale for the geostrophic equilibrium solution as well. That was seen in the adjustment from the initial discontinuity, because the discontinuity did not spread out indefinitely, but only over a distance of the order of the Rossby radius.

For geostrophic flow, the Rossby radius is the scale for which the two contributing terms in (7.2.9) to the perturbation potential vorticity Q' are of the same order. For a sinusoidal variation of surface elevation with wavenumber κ_H, the contribution to Q' from the vorticity ζ is in the ratio

$$-\frac{\zeta}{f} : \frac{\eta}{H} = \kappa_H^2 a^2 : 1 \tag{7.5.1}$$

to the contribution from the surface elevation, by (7.2.19). For short waves ($\kappa_H^{-1} \ll a$) therefore, the vorticity term dominates, whereas the surface elevation term dominates for long waves ($\kappa_H^{-1} \gg a$).

The ratio (7.5.1) gives not only the partition of perturbation potential vorticity, but also the *partition of energy*. This may be seen by multiplying the terms on the left-hand side of (7.5.1) by $\frac{1}{2}\rho g H \eta$ and integrating over a wavelength. The second term

$$\frac{1}{2}\rho g \int\int \eta^2 \, dx \, dy$$

is the potential energy, whereas the first is, by (7.2.19),

$$\begin{aligned} &-\frac{1}{2}\rho\left(\frac{g}{f}\right)^2 H \int\int \eta\left(\frac{\partial^2\eta}{\partial x^2} + \frac{\partial^2\eta}{\partial y^2}\right) dx\, dy \\ &= \frac{1}{2}\rho\left(\frac{g}{f}\right)^2 H \int\int \left\{\left(\frac{\partial\eta}{\partial x}\right)^2 + \left(\frac{\partial\eta}{\partial y}\right)^2 - \frac{\partial}{\partial x}\left(\eta\frac{\partial\eta}{\partial x}\right) - \frac{\partial}{\partial y}\left(\eta\frac{\partial\eta}{\partial y}\right)\right\} dx\, dy \\ &= \frac{1}{2}\rho H \int\int (u^2 + v^2)\, dx\, dy, \end{aligned}$$

the last equality making use of (7.2.14). Thus the first term is the perturbation kinetic energy, and so

$$\text{K.E.} : \text{P.E.} = \kappa_H^2 a^2 : 1, \tag{7.5.2}$$

i.e., short-wavelength geostrophic flow contains mainly kinetic energy, whereas long-wavelength geostrophic flow has most of its energy in the potential form.

Now *typical values* of the Rossby radius will be calculated. These vary somewhat with latitude because of the variation of f that is given by (7.4.1), i.e., by

$$f = 1.47 \times 10^{-4} \sin\varphi \quad \text{s}^{-1}. \tag{7.5.3}$$

Estimates will be based on the value $f = 1.0 \times 10^{-4}\ \text{s}^{-1}$ appropriate to 45° latitude,

but it should be remembered that the Rossby radius is considerably *larger near the equator*, e.g., four times bigger at 10°, where $f = 0.25 \times 10^{-4}\ \text{s}^{-1}$.

For deep water in the ocean, where H is 4 or 5 km, c is about 200 m s^{-1} and therefore the Rossby radius $a = c/f \approx 2000$ km. This is large compared with the depth, so the hydrostatic approximation is valid at this scale, although the scale is rather large for f to be taken as constant. For applications on the continental shelves and in shallow seas like the North Sea much smaller values apply because the depth is much smaller. For $H = 40$ m, for instance, $c = 20$ m s^{-1} and $a = c/f = 200$ km. Since the North Sea has larger dimensions than this, rotation has a strong effect on transient motions such as tides and surges.

The above values are calculated for a homogeneous shallow layer of fluid. However, the adjustment problem can also be done for a stratified fluid using the separation of variables technique discussed in Chapter 6. The Coriolis acceleration has the same structure in the vertical as has the acceleration relative to the rotating frame, so the separation technique works in the same way and the analysis of Sections 7.2 and 7.3 applies to each of the normal modes, the only difference (see Sections 6.11 and 6.14) being that H is replaced by the equivalent depth H_e, which is related to the separation constant c_e by (6.11.14).

Thus there is a Rossby radius associated with each of the normal modes. The values calculated above are for the barotropic mode and are therefore called values of the *barotropic Rossby radius*. Each of the baroclinic modes has an associated Rossby radius

$$a_n = c_n/|f|, \qquad n = 1, 2, \ldots, \tag{7.5.4}$$

which can be called the nth *baroclinic Rossby radius*, c_n being the nth value of the separation constant c_e (see Section 6.11), which is equal to the wave speed of the nth mode in a nonrotating system. If a value of n is not given, the first baroclinic mode is understood. For the ocean, the value of c_1 is usually 1–3 m s^{-1}, so typical values of the baroclinic Rossby radius are 10–30 km, with larger values in low latitudes. This is large compared with the vertical scale (which may be taken as the thermocline depth of about 1 km), so the hydrostatic approximation is valid at this scale. The baroclinic Rossby radius is a natural scale in the ocean that is often associated with boundary phenomena, such as boundary currents and fronts, and with eddies.

For the atmosphere, the Lamb wave is the fastest mode with $c \approx 300$ m s^{-1}. The associated Rossby radius of 3000 km is too large for the f-plane approximation to be valid. For internal modes, there is a continuous set of modes and therefore a continuous set of Rossby radii. In the isothermal case, $c \approx N/m$, where N is the buoyancy frequency and m the vertical wavenumber, so

$$a \approx N/mf. \tag{7.5.5}$$

The ratio N/f is typically of order 100, so the Rossby radius is about 100 times the vertical scale m^{-1}. For a vertical scale associated with the height of the tropopause a is about 1000 km. This is the predominant scale seen on weather charts as the scale of cyclones and anticyclones, and is often called the "synoptic scale."

For both ocean and atmosphere it happens that

$$N \gg f \tag{7.5.6}$$

except for rather limited regions; the horizontal scale a is therefore large compared with the vertical scale m^{-1}, and therefore the hydrostatic approximation is justified for motions with these scales. The fact that (7.5.6) is generally true has strongly influenced the way rotation effects have been introduced in this chapter, in particular, the restriction to motions for which the hydrostatic approximation is valid. For a planet for which (7.5.6) were not true, a rather different approach would be needed.

For baroclinic modes, the results (7.5.1) and (7.5.2) are still valid, but the term involving η is then associated with vertical displacements of isopycnals and in the case of a compressible medium, with compression and expansion of fluid elements, i.e., with changes of internal and potential energy. Thus it can be said that the term represented by η corresponds to changes in the mass field, whereas that represented by ζ corresponds to changes in the velocity field. Thus for large scales ($\kappa_H a \ll 1$) (7.5.1) and (7.5.2) show that the potential vorticity perturbation is mainly associated with perturbations in the mass field, and that the energy changes are in the potential and internal forms. On the other hand, for small scales ($\kappa_H a \gg 1$) potential vorticity perturbations are associated with the velocity field, and the energy perturbation is mainly kinetic. It follows that a distinction can be made between the adjustment processes at different scales. At large scales ($\kappa_H^{-1} \gg a$), it is the mass field that is determined [through (7.2.10)] by the initial potential vorticity, and the velocity field is merely that which is in geostrophic equilibrium with the mass field. It is said, therefore, that the large-scale velocity field adjusts to be in equilibrium with the large-scale mass field. On the other hand, at small scales ($\kappa_H^{-1} \ll a$) it is the velocity field that is determined by the initial potential vorticity, and the mass field is merely that which is in geostrophic equilibrium with the velocity field. In this case it can be said that the mass field adjusts to be in equilibrium with the velocity field.

7.6 The Geostrophic Balance

An important feature of the response of a rotating fluid to gravity is that it does not adjust to a state of rest, but rather to a geostrophic equilibrium [the name geostrophic is due to Shaw (1916)]. Consequently, the ocean and atmosphere tend to be close to a state of geostrophic equilibrium all the time [see Phillips (1963) for a review].

The development of an awareness of this fact has been very slow. The barometer was invented by Torricelli in 1643, and its potential for weather prediction was soon realized. Barometer readings, along with temperature, wind direction, and state of the sky, were taken daily in the first network of stations set up by Anitoni, secretary to the Grand Duke Ferdinand II of Tuscany in 1654 [see, e.g., Khrgian (1970, Chapter 6)]. This network included stations as far apart as Florence, Warsaw, and Paris and operated until 1667. Various other attempts were made in the eighteenth century, the most notable being an international effort with standardized instruments organized by the Mannheim (or Palatine) Meteorological Society, beginning in 1781.

However, a clear idea of the relationship between wind direction and pressure gradient does not appear to have emerged until 200 years after the invention of the barometer. Many writers in the mid-nineteenth century showed some awareness of the relationship, so one cannot easily associate the idea with any particular person. Hildebrandsson and Teisserenc de Bort (1898, Chapter 3) give examples, the earliest being Brandes (1820), who studied data collected by the Mannheim Society for the year 1783. He did not publish diagrams, but Fig. 7.6 shows a chart constructed from Brandes' figures by Hildebrandsson and Teisserenc de Bort. Contours are pressure deviations in lines ($\frac{1}{12}$ Parisian inch of mercury or about 3 mb) from mean values at each locality. Brandes noted that the wind direction was closely related to the pressure distribution and attributed the turning to the right (from the direction opposite to the pressure gradient) to the rotation of the earth. Another interesting example is shown in Fig. 7.7 from Birt (1847). In the first report of the British Association in 1832, Forbes expressed his hopes for future networks of meteorological stations as a means for detecting "great atmospheric tidal waves" like those treated by Laplace. As a result, a committee was set up under Herschell, and Birt gave five reports on work he did for the committee. Birt was influenced by Scott Russell's report on waves (1844), referred to in Section 5.4, and proposed that the wave description shown in Fig. 7.7 could explain much of the available observations.

Let the strata *aaa'a'*, *b' b' bb*, fig. 2, represent two parallel aerial currents, *aaa'a'* being from S.W. and *b' b' bb* from N.E., and conceive them both to advance from

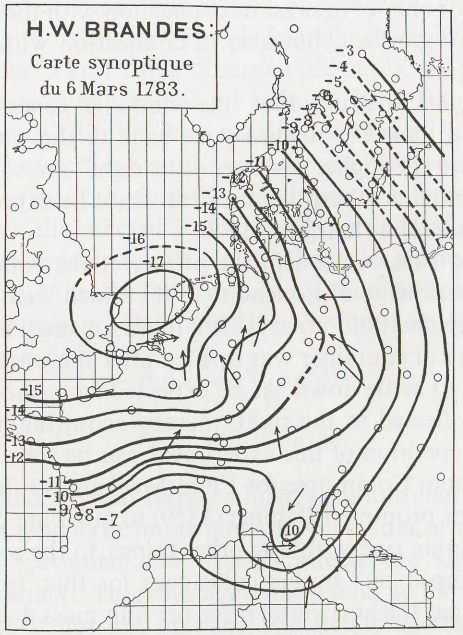

Fig. 7.6. A reconstruction by Hidebrandsson and Teisserenc de Bort (1898) of the early synoptic maps of Brandes (1820), based on data collected by the Mannheim Society. The contours are of pressure deviation from the mean value in lines ($\frac{1}{12}$ of a Parisian inch or about 3 mb), and the arrows show wind direction.

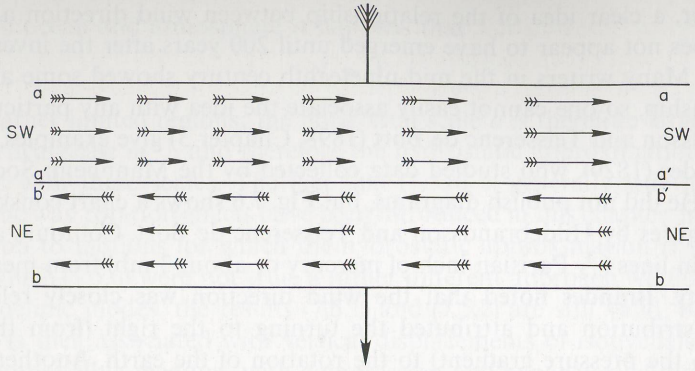

Fig. 7.7. A wave description of wind and pressure changes proposed by Birt (1847 fig. 2), which included the concept of wind being along isobars. The lines aa and bb are lines of low pressure, whereas the line a'a' or b'b' is one of high pressure. Winds in between are in the direction shown, and the whole system propagates in the direction shown by the large arrow.

> the N.W. in the direction of the large arrow, that is the strata themselves will advance with a *lateral* motion. Now conceive the barometer to commence rising just as the edge *bb* passes any line of country, and continue rising until the edge *b'b'* arrives at that line, when the maximum is attained. The wind now changes and the barometer immediately begins to fall and continues to fall until the edge *aa* coincides with the line of the country on which *bb* first impinged (Birt, 1847 p. 135).

Birt's description is not only of interest in connection with the relation between wind direction and pressure gradient, but also in connection with waves, which will be studied in later chapters.

Despite these insights, the rules that "the wind is in general perpendicular to the barometric slope" and that "if you turn your back to the wind, the lower pressure will be on your left and the higher pressure your right" are sometimes referred to as Buys-Ballot's law (for the northern hemisphere) since he expressed them thus in his yearbooks of 1857 and 1860 (Khrgian, 1970).

On the theoretical side, interest in the effects of the rotation of the earth was stimulated by the experiments of Foucault (1851), which were followed 8 years later by the "bathtub" experiment of Perrot (1859). In this, a small hole in the center of the base of a large cylindrical container was opened after the water in the container had been left a whole day to settle down. As he expected from theory, Perrot found that fluid particles were deflected to the right, thereby acquiring, in modern parlance, a cyclonic rotation. A repetition of this experiment can be seen in the film "Vorticity" by Shapiro [see National Committee for Fluid Mechanics Films (1972, pp. 63–74)].

Perrot's experiment prompted Babinet (1859) to attribute preferential erosion on the right banks of Siberian rivers, among other things, to the rotation of the earth. He was immediately "jumped on" by his colleagues for this. In particular, Delaunay (1859), after showing that the horizontal force per unit mass due to rotation is f times the velocity, put it this way: Consider a straight canal in the northern hemisphere. If the fluid is at rest it will exert equal pressures on its two banks. If it moves, "the pressure will diminish a little on the bank left of the current and increase a little on the right bank (p. 692)." He also said that the changes would be quite small. Combes (1859) went further and showed that the surface would slope up to the right in the northern hemisphere (and to the left in the southern hemisphere) with an inclination given by

$$\text{surface slope} = 2\Omega \sin \varphi \, v/g, \tag{7.6.1}$$

which is another way of expressing the geostrophic balance (7.2.14). He calculates that for a river 4 km wide flowing at 3 m s^{-1} at 45° latitude, the difference in level between the two sides would be 12 cm.

These discussions at the Paris Academy were not directed toward meteorological questions, but had some "spinoff" in European meteorology later [see Abbe (1877, 1893, 1910)]. In the United States at this time, however, Ferrel was concerned with applying the equations of fluid motion on a rotating sphere to meteorological problems, and in particular to the global circulation. He appears to be the first person (Ferrel, 1859, pp. 397–398) to deduce that large-scale motions of the atmosphere are approximately hydrostatic and geostrophic. His approach was to first integrate the hydrostatic equation, neglecting changes of temperature with height to obtain the exponential falloff (3.5.12) with height. This was substituted in the north–south component (4.12.15) of the momentum equation and then approximations were made that amount to approximating (4.12.15) by

$$2\Omega u \sin \varphi = -(\rho r)^{-1} \partial p/\partial \varphi + \text{friction term}. \tag{7.6.2}$$

He then argued that the friction term would be relatively small and used surface pressure measurements to calculate from his formula the zonal winds at the surface and at a height of 3 miles (5 km), using observed pressures and a reasonable approximation for dependence of temperature on latitude. At 5 km he obtained westerly (i.e., eastward) winds at all latitudes with maxima of 13 m s^{-1} at 55°N and 23 m s^{-1} at 40°S. He did not find easterlies near the equator as observed (see Fig. 7.9), but as he stated: "Very near the equator the formula ... fails practically, since, on account of the small value of sin φ there, the effect of" friction and inertia "may be very great" (p. 401).

The geostrophic relationship found in (7.2.14) applies to any one mode. The more general result (which could be obtained by adding contributions from modes) comes from balancing the pressure gradient and Coriolis terms in (4.10.11) to give

$$-fv = -\rho^{-1} \partial p/\partial x, \tag{7.6.3}$$

$$fu = -\rho^{-1} \partial p/\partial y. \tag{7.6.4}$$

The nonlinear terms and friction terms, which were automatically excluded in the linear inviscid analysis, tend to be important only in regions of strong gradient such as fronts and boundary currents, and friction effects are significant, though not dominant, near the surface. Thus surface winds tend to be along isobars, in the direction given by Buys-Ballot, and pressure is related to a stream function by (7.2.18), i.e., winds are strongest when isobars are closest together. Another way of remembering direction is in terms of the direction of rotation around a "high" (anticyclone) or "low" (cyclone). The air has a cyclonic rotation around a cyclone, as the term

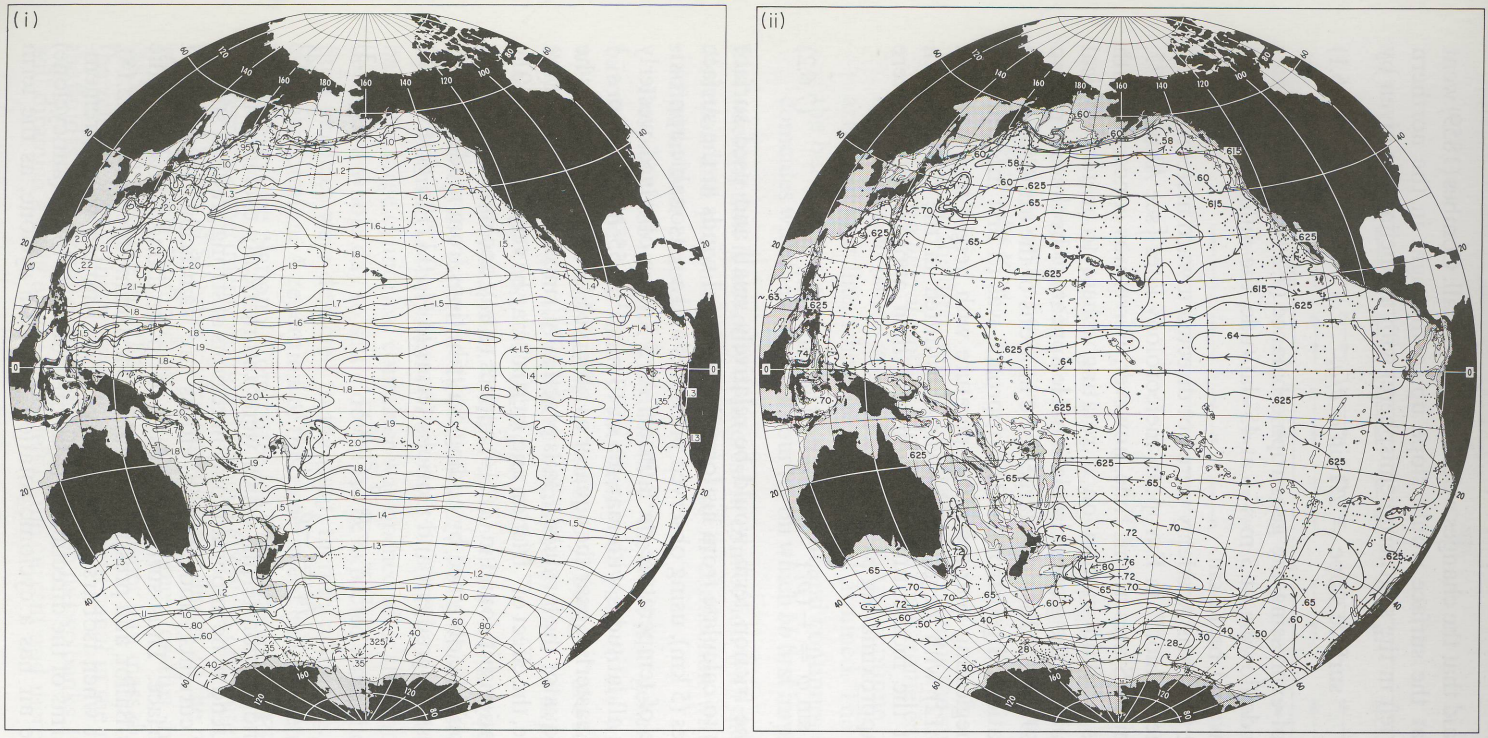

(a)

Fig. 7.8. (a) (i) The dynamic height of the sea surface of the Pacific Ocean *relative* to 1000 db (i.e., the anomaly in the difference of geopotential between these two pressure levels) in dynamic meters. Arrows show the direction of the current at the surface relative to that at 1000 db. Dots represent data points where values were computed. [From Reid and Arthur (1975, Fig. 1).] (ii) A similar map, showing the dynamic height or geopotential anomaly of the 1000-db surface *relative* to 2000 db. Oceanographers make use of these charts for inferring currents because of the difficulties involved in determining the absolute topography of a pressure surface. (b) Thickness charts give the equivalent information for the atmosphere, e.g., (i) shows the wintertime difference in geopotential height (m) between the 850- and 1000-mb surfaces. Values can be converted into average temperature between the two levels in K by multiplying by 0.210. The contour interval is 10 m (2.1 K). Because the field is so nearly zonal, certain features are best brought out by plotting departures from the zonal mean as is done in (ii). The contour interval is now 9 m (1.9 K), and the difference between the warmth of the oceans and coldness of the continents is apparent. There is no need to use such charts to infer winds since the height of pressure surfaces can be directly measured. For example, (iii) shows the wintertime mean height (m) of the 200-mb surface where winds are near their maximum values. The contour interval is 100 m. *[All three figures are courtesy of G. H. White and are based on NMC data compiled by N.-C. Lau].*

(b) (ii)

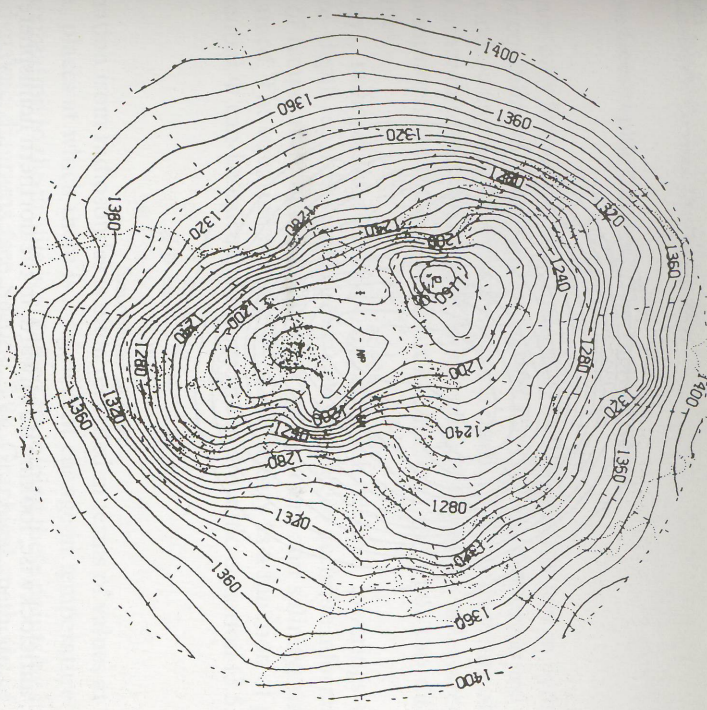

(b) (i)

Fig. 7.8. *(continued)*

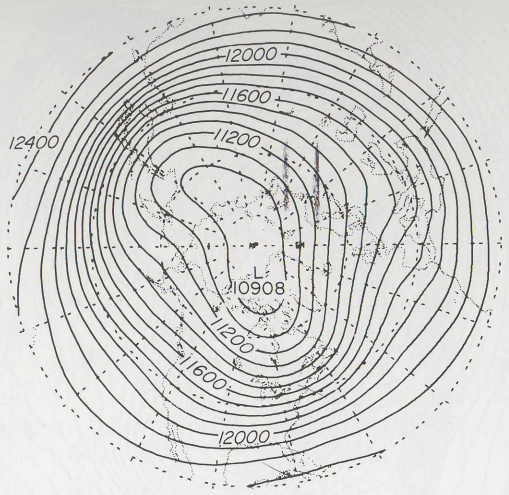

Fig. 7.8. *(continued)*

implies (i.e., anticlockwise, looking downward, in the northern hemisphere and clockwise in the southern hemisphere) and anticyclonic rotation around an anticyclone.

There is a significant correction to geostrophy for surface winds. One way of expressing this is to define the *geostrophic wind* (u_g, v_g) by

$$fu_g = -\rho^{-1}\,\partial p/\partial y, \qquad fv_g = \rho^{-1}\,\partial p/\partial x, \tag{7.6.5}$$

and express the surface wind in terms of the geostrophic wind. This amounts to a reduction in magnitude (which increases as the distance from the ground decreases) and a change in direction toward the low pressure, typical angles being around 20°. In practice, the correction depends on stability of the air and on whether or not equilibrium conditions have been established. (Diurnal variations in heating rate and variations in terrain work against this over land.) The deviation from geostrophy decreases with height and is usually quite small above 1 km. A verification of the closeness of geostrophic balance aloft was obtained by Gold (1908).

Although (7.6.3) and (7.6.4) are a convenient way of expressing the geostrophic relationship at the surface, a more convenient form for other levels is in terms of isobaric coordinates (see Section 6.17), i.e., the velocity on a constant-pressure surface is given by

$$-fv = -\partial\Phi/\partial x, \tag{7.6.6}$$

$$fu = -\partial\Phi/\partial y, \tag{7.6.7}$$

where Φ is the geopotential on that surface. This is the form used in practice in both meteorology and oceanography. The advantage in meteorology is clear because density is eliminated and thus charts of Φ at different pressure levels have the same scale for converting into velocities. As an example, Fig. 7.8b includes charts of the geopotential height (see Section 3.5) of the 200 mbar surface. Winds at this pressure can be calculated from (7.6.6), (7.6.7), and (3.5.2).

7.7 Relative Geostrophic Currents: The Thermal Wind

Ferrel not only found that the atmosphere was approximately in hydrostatic and geostrophic equilibrium, but also showed that this fact could be exploited to calculat upper air winds, using surface pressure measurements and temperature observations For lack of other information, Ferrel's winds at an elevation of 3 miles were calculated on the assumption that temperatures up to this level were not too different from surface values.

Nowadays, radiosonde ascents of the atmosphere (and lowerings of salinity-temperature–depth recorders in the ocean) are routine, so accurate information abou variations of temperature and humidity (or temperature and salinity) with pressur can be obtained. The equation of state gives the density as a function of pressure, s the geopotential Φ can be calculated from the hydrostatic equation (3.5.6), i.e.,

$$d\Phi = -\frac{dp}{\rho} = -v_s\,dp. \tag{7.7.1}$$

The information from radiosondes is often recorded in terms of values at "significan points," i.e., places at which there is a significant change in temperature gradient. A good approximation to the profile is obtained by joining these points by straight line on thermodynamic diagrams (see Section 3.9). Graphical methods of calculatin geopotential changes from these diagrams are discussed, e.g., by Godske *et al.* (195 Chapter 3).

In the atmosphere, the dynamic height of any pressure surface can be calculate because the surface pressure is known. The same is not true in the ocean because th elevation of the free surface relative to a geopotential is not usually known. Howeve differences in the dynamic height of given pressure surfaces can still be calculated, s the geostrophic velocity at one level can be calculated relative to that at another.

Temperature and salinity values in the ocean, if obtained by STD (salinity temperature–depth) or CTD (conductivity–temperature–depth) recorders, ar usually listed in a cruise report and sent to a data center as values at certain standar depths, with some additional values where changes of gradient occur. If obtained b Nansen bottles, which record temperatures and collect samples of water for analys at prearranged depths, values at those depths are given. There are standard compute routines to calculate values of density and of dynamic height. For calculations of th latter quantity, the density is calculated in terms of the *specific volume anomaly* defined as the specific volume $v_s = \rho^{-1}$ related to the value at the same pressure fo a temperature of 0°C and a practical salinity of 35, i.e.,

$$\delta = v_s(S, T, p) - v_s(35, 0, p). \tag{7.7.2}$$

δ can be calculated using (A3.3), and is usually given in units of 10^{-8} m^3 kg^{-1}. Th geopotential anomaly Φ' (the usual notation is $-\Delta D$) is then defined by

$$\Delta D = -\Phi' = \int_0^p \delta\,dp, \tag{7.7.}$$

i.e., is obtained by integration from zero pressure (the surface) to the pressure co cerned. Since the anomalies are expressed relative to a function of pressure only, th

horizontal gradients of Φ' along isobaric surfaces are the same as horizontal gradients of Φ. Hence

$$-f\{v_g(p) - v_g(0)\} = -\frac{\partial \Phi'(p)}{\partial x},$$
$$f\{u_g(p) - u_g(0)\} = -\frac{\partial \Phi'(p)}{\partial y}, \tag{7.7.4}$$

give geostrophic currents relative to the surface. Similarly, geostrophic velocities at pressure p_1 can be calculated relative to another pressure p_2 by

$$-f\{v_g(p_1) - v_g(p_2)\} = -\frac{\partial}{\partial x}\{\Phi'(p_1) - \Phi'(p_2)\},$$
$$f\{u_g(p_1) - u_g(p_2)\} = -\frac{\partial}{\partial y}\{\Phi'(p_1) - \Phi'(p_2)\}. \tag{7.7.5}$$

Usually the reference level (subscript 2) is chosen to be the *lower* of the two levels, and hence at the higher pressure ($p_2 > p_1$).

As an example, Fig. 7.8a shows the dynamic topography of (i) the surface of the Pacific Ocean relative to the 1000-decibar level and (ii) the 1000-db relative to the 2000-db level. [In oceanography the *decibar* (dbar) (see Section 3.5) is often used as a unit of pressure since a pressure change of 1 db corresponds to a change of depth of $1/\rho g$ times this value, which is very close to 1 m: typically 1 db = 0.995 m near the surface and 0.969 m at the 5000-db level. Often the distinction between a decibar and a meter is of little importance and is ignored.] Usually, currents at the deeper levels are small compared with surface values, so the surface currents relative to 1000 or 2000 db are assumed to be a good approximation to actual surface currents. There is always the question, however, of which reference level gives the best approximation to surface currents. The ideal reference level would be a "level of no motion," but such a level does not necessarily exist in practice because *both* components of velocity need to vanish at the same level. Methods of deducing a reference level from temperature and salinity observations in a neighborhood are discussed by Stommel and Schott (1977) and Killworth (1980b).

In meteorology, the dynamic height of one pressure surface relative to another is called the *thickness*. If the perfect gas law (3.1.2) is satisfied, (7.7.1) gives

$$\Phi_1 - \Phi_2 = \int_{p_1}^{p_2} p^{-1} RT\, dp = R\overline{T} \ln(p_2/p_1), \tag{7.7.6}$$

where $\overline{T}$ is the temperature averaged with respect to the logarithm of the pressure between the two levels. Hence the thickness, and therefore relative winds, is associated with a mean temperature $\overline{T}$. Another interpretation of $\overline{T}$ is obtained by integrating the hydrostatic equation in the form (3.5.11), which gives

$$\ln(p_2/p_1) = \int_{p_2}^{p_1} (g/RT)\, dz = (g/R\overline{T}) \int_{p_2}^{p_1} dz, \tag{7.7.7}$$

i.e., $1/\overline{T}$ is the reciprocal of the temperature averaged with respect to distance z

between the two pressure surfaces. Figure 7.8b shows an example of a thickness chart. In meteorology these are more often used as a measure of mean temperature than of relative winds.

In the above discussion, the information in the hydrostatic and geostrophic equations has been combined, following Ferrel, by first integrating the hydrostatic equation and then using the geostrophic relation. Alternatively, the geostrophic equations (7.6.6) and (7.6.7) can be differentiated with respect to pressure and then the hydrostatic relation used to substitute for $\partial\Phi/\partial p = -\rho^{-1}$. The result is

$$f\,\partial v/\partial p = \rho^{-2}\,\partial\rho/\partial x, \qquad f\,\partial u/\partial p = -\rho^{-2}\,\partial\rho/\partial y. \tag{7.7.8}$$

Alternatively, using the hydrostatic equation again to put $dp = -\rho g\, dz$, this may be written

$$f\,\partial v/\partial z = -g\rho^{-1}(\partial\rho/\partial x)_p, \qquad f\,\partial u/\partial z = g\rho^{-1}(\partial\rho/\partial y)_p, \tag{7.7.9}$$

where the derivatives on the right-hand side are taken on constant-pressure surfaces. (The difference between the gradients on constant-pressure and constant-level surfaces is usually so small that the distinction is unimportant for practical purposes.)

For a perfect gas $\rho = p/RT$, so the derivatives on the right can be reexpressed in terms of temperature to give

$$f\,\partial v/\partial z = gT^{-1}(\partial T/\partial x)_p, \qquad f\,\partial u/\partial z = -gT^{-1}(\partial T/\partial y)_p. \tag{7.7.10}$$

This form of the equation is called the *thermal wind* equation, and gives a relation between temperature gradient (on an isobaric surface) and wind shear. It follows that, as Ferrel found, when temperature decreases toward the poles, winds become more westerly (i.e., stronger toward the east) with height. Figure 7.9 shows observed distributions of temperature and wind with latitude and height, and the relationship between the two fields, as expressed by (7.7.10), is apparent.

It is useful to think of the thermal wind as the wind at one level (denoted by subscript 1, say) *relative to* the wind at a *lower* level (denoted by subscript 2). Then the thermal wind blows along isotherms (or, more precisely, along contours of constant thickness) with, in the northern hemisphere, *cold* air on the *left* and warm air on the right. There are various consequences that are useful to remember.

Suppose, for instance, the geostrophic wind at the reference level has a component from cold to warm. Then the thermal wind will be directed to the left in the northern hemisphere (see Fig. 7.10), so the wind will *back* with height (i.e., the wind vector will rotate anticlockwise, or cyclonically, with height). Conversely, the wind will *veer* with height (i.e., rotate anticyclonically) if the wind has a component from warm to cold. Thus, *backing* of the wind with height is associated with cold air advection and veering with height is associated with warm air advection.

On a chart showing isotherms on a constant-pressure surface, the shear vector is directed cyclonically around low temperatures (or low thickness) and anticyclonically around high temperatures (or high thickness). Thus if a *low*-pressure disturbance has a *cold* core, the cyclonic flow around the core will *increase* with height, and vice versa. Similarly, if a high-pressure disturbance has a warm core, the anticyclonic flow will increase with height, and vice versa. If temperature and pressure centers do not

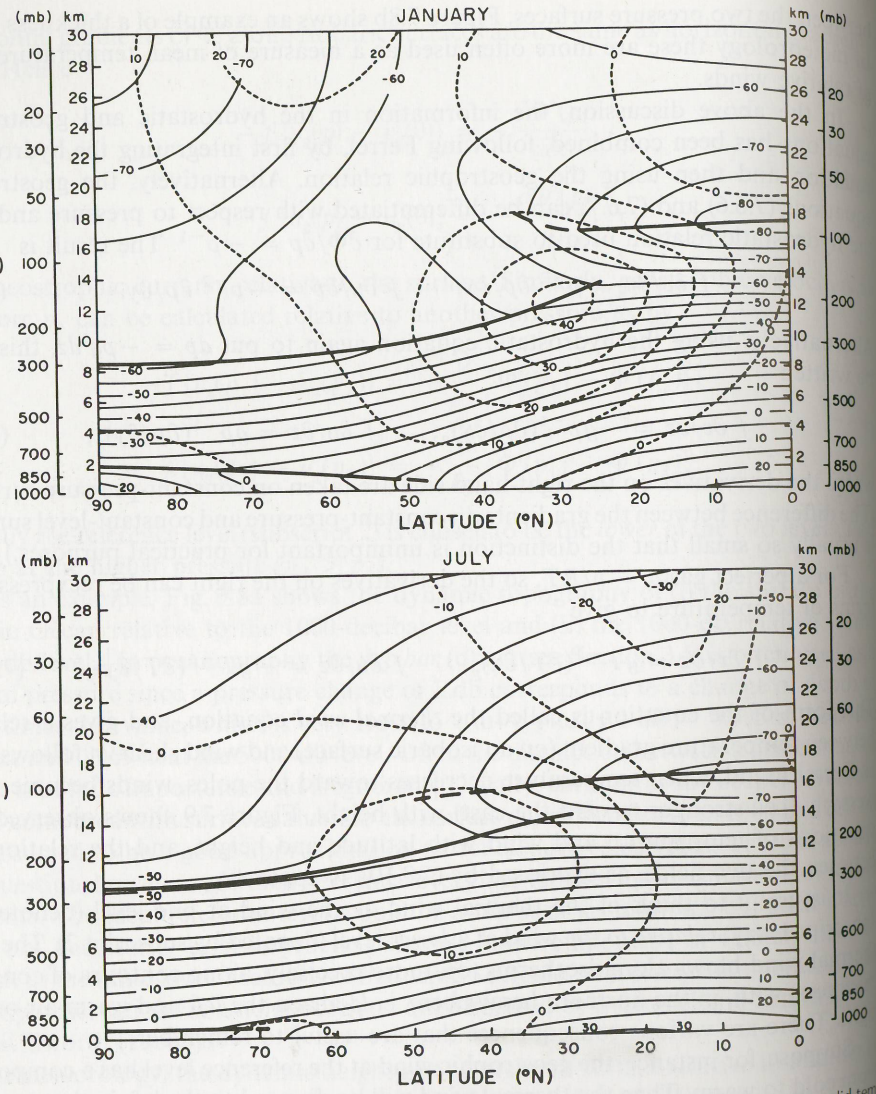

Fig. 7.9. Mean meridional cross sections of wind and temperature for (a) January and (b) July. Thin solid temperature lines are in degrees Celsius and dashed wind speed lines are in meters per second. Heavy solid lines represent tropopause and inversion discontinuities. [After *Active Forecast Guide*, Navy Weather Research Facility, April 1962.]

coincide, the *cyclones* will *shift* with height *toward cold air*, and anticyclones will shift toward warm air.

For the ocean, the equation of state can be used to give the density gradients in (7.7.9) in terms of temperature and salinity gradients. This gives (see Section 3.6)

$$f\,\partial v/\partial z = g\alpha\,\partial T/\partial x - g\beta\,\partial s/\partial x, \qquad f\,\partial u/\partial z = -g\alpha\,\partial T/\partial y + g\beta\,\partial s/\partial y. \tag{7.7.11}$$

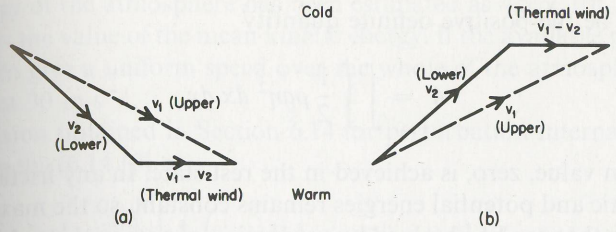

Fig. 7.10. The association between the direction of rotation of the wind vector with height and the direction of heat advection. Subscript 2 denotes the lower level and subscript 1 the upper level. In the northern hemisphere, cold air is on the left of an observer traveling with the thermal wind $v_1 - v_2$. Consequently, cold air advection [case (a)] corresponds to a wind vector that backs (i.e., rotates cyclonically) with height, whereas warm air advection [case (b)] is associated with a wind vector that veers (i.e., rotates anticyclonically) with height in the northern hemisphere.

Alternatively (see Section 3.7), T can be replaced by potential temperature θ and α, β by α', β'. When salinity gradients are small and temperature decreases toward the poles, currents become more strongly westward with depth. A manifestation of this result is in the poleward displacement with depth of the centers of the subtropical gyres, which are anticyclonic. This can be seen in Fig. 7.8a.

A limiting form of the thermal wind is obtained in the case of a "front" or sloping surface of discontinuity of density. If this surface is given by $z = h(x, y)$, subscript 2 denotes values *below* the surface, and subscript 1 values above, then the additional pressure created below the surface by the discontinuity will be

$$p_2 - p_1 = (\rho_2 - \rho_1)g(h - z) \tag{7.7.12}$$

by the hydrostatic equation. From the geostrophic relation, the additional velocity *below* the surface will be given by

$$f(v_2 - v_1) = g'\,\partial h/\partial x, \qquad f(u_2 - u_1) = -g'\,\partial h/\partial y, \tag{7.7.13}$$

where

$$g' = (\rho_2 - \rho_1)g/\rho_2. \tag{7.7.14}$$

Thus the additional velocity is directed along contours of the surface of discontinuity and has magnitude g'/f times the slope of the surface. A special case is the discontinuity at a free surface, in which (7.7.13) reduces to the result (7.6.1) obtained by Combes (1859). The relation (7.7.13) for a general surface of discontinuity is often referred to as Margules' (1906) relation. A more general form of the relation for zonal flows was obtained by Helmholtz (1888).

7.8 Available Potential Energy

In Section 5.7, the energy changes associated with the adjustment under gravity of a homogeneous fluid were considered for the case of small perturbations from a state of rest. The perturbation potential energy associated with the surface elevation